

Possibility of valence-fluctuation mediated superconductivity in Cd-doped CeIrIn₅ probed by In-NQR

M. Yashima,^{1,2} N. Tagami,¹ S. Taniguchi,¹ T. Unemori,¹ K. Uematsu,¹
H. Mukuda,^{1,2} Y. Kitaoka,¹ Y. Ōta,³ F. Honda,³ R. Settai,³ and Y. Ōnuki³

¹*Department of Materials Engineering Science, Osaka University, Osaka 560-8531, Japan*

²*JST, TRiP (Transformative Research-Project on Iron Pnictides), Chiyoda, Tokyo 102-0075, Japan*

³*Department of Physics, Graduate School of Science, Osaka University, Osaka 560-0043, Japan*

We report on a pressure-induced evolution of exotic superconductivity and spin correlations in CeIr(In_{1-x}Cd_x)₅ by means of In-Nuclear-Quadrupole-Resonance (NQR) studies. Measurements of an NQR spectrum and nuclear-spin-lattice-relaxation rate $1/T_1$ have revealed that antiferromagnetism induced by the Cd-doping emerges locally around Cd dopants, but superconductivity is suddenly induced at $T_c = 0.7$ and 0.9 K at 2.34 and 2.75 GPa, respectively. The unique superconducting characteristics with a large fraction of the residual density of state at the Fermi level that increases with T_c differ from those for anisotropic superconductivity mediated by antiferromagnetic correlations. By incorporating the pressure dependence of the NQR frequency pointing to the valence change of Ce, we suggest that unconventional superconductivity in the CeIr(In_{1-x}Cd_x)₅ system may be mediated by valence fluctuations.

Cerium (Ce)-based heavy-fermion compounds, CeMIn₅ (M = Co, Rh, and Ir), provide us with the opportunity to systematically investigate the interplay between antiferromagnetism (AF) and superconductivity (SC) [1–4]. CeIrIn₅ and CeCoIn₅ show SC at ambient pressure (P) below $T_c = 0.4$ and 2.3 K, respectively [1–4]. In CeRhIn₅, which is an antiferromagnet with $T_N = 3.8$ K at ambient P , SC occurs at $T_c \sim 2.2$ K under P over 2.1 GPa. However, it has been suggested that the superconducting nature in CeIrIn₅ should be distinguished from those in CeCoIn₅ and CeRhIn₅ from several points of view. The existence of two superconducting phases was reported in CeRh_{1-y}Ir_yIn₅ [5]. Figs.1(a) and 1(b) show the respective phase diagrams of SC (denoted as SC1 and SC2) for CeRh_{1-y}Ir_yIn₅ and CeIrIn₅ under P . SC1 is closely related to antiferromagnetic (AFM) correlations, as argued extensively in CeCoIn₅[6] and CeRhIn₅[7], whereas it is reported from the previous NQR measurements that the SC2 in CeIrIn₅ occurs in a different situation from SC1 as follows [8]. The maximum of $T_c \sim 1$ K around 3 GPa takes place under the absence of AFM correlations that is suggested by the fact that the $(T_1T)^{-1}$ -constant behavior, which is an order of magnitude suppressed by P , is observed above T_c . Here, T_1 is a nuclear-spin-lattice-relaxation time. However, the values of $(T_1T)^{-1}$ are an order of magnitude larger than those in LaIrIn₅, indicating that nearly wave-number independent magnetic and/or valence fluctuations are dominant under high P . Actually, the large electronic specific heat coefficient $\gamma \sim 0.38$ J/molK² at $P = 1.56$ GPa is observed in CeIrIn₅ [9]. Moreover, from the resistivity measurements, a non-Fermi liquid behavior that the resistivity approximately follows a $T^{1.5}$ law has been observed in the wide P range of 0 to 3.1 GPa [3].

Furthermore, we note that SC2 does not occur in the high P region in CeRh_{0.4}Ir_{0.6}In₅, while SC1 is observed in the low P region, as shown in Fig. 1(d). These results suggest that SC2 is discontinuous with SC1 and hence the substitution of Rh for Ir does not correspond to the application of P in CeIrIn₅. Therefore, it is anticipated that the superconducting mechanism of SC2 differs from that of SC1.

Meanwhile, it was reported that all the anomalous transport properties observed in CeRh_{0.2}Ir_{0.8}In₅(SC1) and CeIrIn₅(SC2) originate from the AFM spin fluctuations irrespective of the superconducting phase to which the system belongs. [10]. In this context, the reason why the maximum T_c of SC2 in CeIrIn₅ is realized far away from an AFM quantum critical point (QCP) is still an underlying issue. The existence of SC1 and SC2 was first reported in CeCu₂(Si_{1-x}Ge_x)₂ [11]. It is suggested from extensive experimental and theoretical studies that SC2 emerging in the high P region is mediated by valence fluctuations [12–15]. In order to develop insight into SC2, we report on the P -induced evolution of unique SC characteristics in pure and Cd-doped CeIrIn₅.

Single crystals of CeIr(In_{1-x}Cd_x)₅, CeRh_{1-y}Ir_yIn₅, and CeCo(In_{0.9}Cd_{0.1})₅ grown by the self-flux method were crushed into coarse powder in order to allow the RF pulses to easily penetrate the sample for NQR measurements. Here T_c 's for the samples are determined by a sudden decrease in nuclear-spin-lattice-relaxation rate $1/T_1$ below T_c . Hydrostatic P was applied by utilizing a NiCrAl-BeCu piston-cylinder cell filled with Daphne 7474 as a P -transmitting medium [16]. To calibrate P at low temperatures, the shift in T_c of Sn metal at P was monitored by resistivity measurements. CeMIn₅ consists of alternating layers of CeIn and MIn₄, and there are

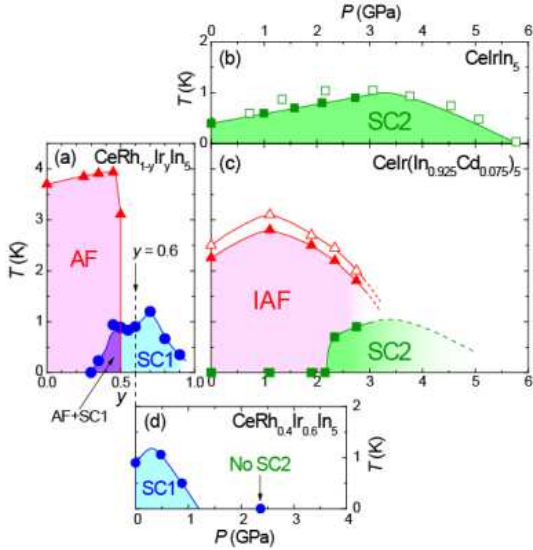


FIG. 1: (Color online) (a) The phase diagram for $\text{CeRh}_{1-x}\text{Ir}_x\text{In}_5$ as a function of Ir concentration. T_N and T_c are referred from Refs. [26, 27]. SC1 is expected to be mediated by magnetic correlations. The length of the horizontal axis between $y = 0$ and 1 is adjusted to coincide with that between 0 and 3 GPa in the other figures. (b) The pressure(P)-temperature(T) phase diagram for CeIrIn_5 [8]. The open squares are referred from the resistivity measurement [3]. SC2 is expected to be mediated by valence fluctuations. (c) The $P - T$ phase diagram for $\text{CeIr}(\text{In}_{0.925}\text{Cd}_{0.075})_5$ which was determined by the present experiment. The T_N (solid) and T'_N (open triangles) are determined from the peak in the T dependence of $1/T_1$ and the broadening of NQR spectrum due to the onset of the AFM order, respectively. (d) The $P - T$ phase diagram for $\text{CeRh}_{0.4}\text{Ir}_{0.6}\text{In}_5$ obtained from the T_1 measurements.

two sites—In(1) and In(2)—per unit cell. The In(1) and In(2) sites are located in the CeIn and MIn_4 layers, respectively. The measurements of an $^{115}\text{In}(I = 9/2)$ -NQR spectrum and $1/T_1$ were mainly performed at the transition of $2\nu_Q$ for the high symmetry In(1) site in CeMIn_5 . T_1 was measured by the conventional saturation-recovery method. When the system is near the AFM QCP, the relations of $(T_1T)^{-1} \propto \chi_Q(T)^n$ ($n = 1/2$ or 1) for the 2- or 3-dimensional AFM spin-fluctuation models are predicted, respectively [17]. Since the staggered susceptibility follows the Curie-Weiss law as $\chi_Q(T) \propto 1/(T + \theta)$, the increase in $(T_1T)^{-1}$ with decreasing T is observed near the AFM QCP. Here, an NQR frequency (ν_Q) is defined by the NQR Hamiltonian, $\mathcal{H}_Q = (h\nu_Q/6)[3I_z^2 - I(I+1) + \eta(I_x^2 - I_y^2)]$, where η is the asymmetric parameter of the electric field gradient [$\eta = 0$ at the In(1) site].

Figure 2(a) shows the T dependence of $(T_1T)^{-1}$ in CeIrIn_5 and $\text{CeIr}(\text{In}_{0.925}\text{Cd}_{0.075})_5$. The AFM order induced by the Cd-doping into the CeMIn_5 system was reported from the specific-heat measurements [18]. In fact, the onset of AFM for $\text{CeIr}(\text{In}_{0.925}\text{Cd}_{0.075})_5$ is corroborated by the observation of a peak in $(T_1T)^{-1}$ at $T_N \sim 2.3$ K as shown in Fig. 2(a). The T dependence of $(T_1T)^{-1}$ above T_N for the Cd-doped sample almost co-

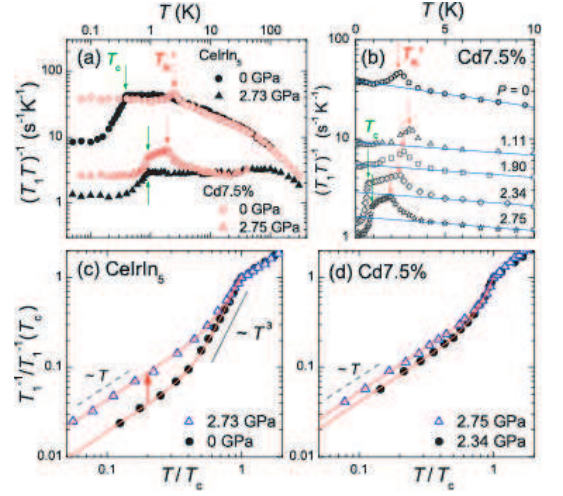


FIG. 2: (Color online) (a) The T dependences of $(T_1T)^{-1}$ for CeIrIn_5 and $\text{CeIr}(\text{In}_{0.925}\text{Cd}_{0.075})_5$. (b) The T dependences of $(T_1T)^{-1}$ at several pressures in the P range of 0 – 2.75 GPa in $\text{CeIr}(\text{In}_{0.925}\text{Cd}_{0.075})_5$. To prevent data points from overlapping, the $(T_1T)^{-1}$ results at 2.34 and 2.75 GPa are divided by 1.5 and 2.4, respectively. (c) The T dependence of $1/T_1$ normalized at T_c at $P=0$ and 2.73 GPa in CeIrIn_5 . (d) The T dependences of $1/T_1$ normalized at T_c at $P=2.34$ and 2.75 GPa in $\text{CeIr}(\text{In}_{0.925}\text{Cd}_{0.075})_5$.

incides with that for the pure one. The effect of the Cd-doping would be local in the normal state, as reported in the previous NQR measurements in Cd-doped CeCoIn_5 [19]. This result suggests that Cd acts as a local defect that nucleates droplets of local AFM order in a system close to an AFM QCP.

Figs.3(a) and 3(b) show the NQR spectra for $3\nu_Q$ at the In(2) site above and below T_N in $\text{CeIr}(\text{In}_{0.925}\text{Cd}_{0.075})_5$ and $\text{CeCo}(\text{In}_{0.9}\text{Cd}_{0.1})_5$, respectively. A clear splitting into two NQR spectra indicates the occurrence of a homogeneous AFM order with a uniform magnetic moment M_{AF} over the whole sample in Cd-doped CeCoIn_5 , as presented in Ref. [19]. In Cd-doped CeIrIn_5 , however, the NQR spectrum below T_N exhibits no clear splitting, but a large broadening at its tail, indicating an inhomogeneous AFM order (IAF) with a large distribution of M_{AF} . This difference in the character of the AFM order is probably relevant to the fact that CeCoIn_5 is much closer to an AFM QCP than CeIrIn_5 . In order to explain the spectral shape for IAF, we assume that the magnitude of M_{AF} at each Ce site depends on the density of Cd dopants surrounding it, as shown in Fig. 3c. We adopt a simple square lattice model (500×500) under randomly distributed 7.5% Cd dopants and a spatial distribution of M_{AF} at each Ce site is given by $M_{AF}^{i,j} \propto \sum_{k,l} \exp(-\frac{|\vec{r}_{k,l} - \vec{r}_{i,j}|^2}{\xi^2})$, where (i, j) and (k, l) indicate positions of Ce and Cd ions, respectively, and ξ is a length that the influence of Cd dopants reaches. Incorporating some local effect of the Cd-doping, a Gaussian function is tentatively assumed to calculate $M_{AF}^{i,j}$. The distribution of M_{AF} obtained from this model with

$\xi = 1.4a$ (a is the lattice parameter of a-axis) is shown in the inset of Fig. 3d. The reproducibility for the distribution of M_{AF} was confirmed due to the sufficiently large size of a 500×500 square lattice. The simulated spectral shape for $3\nu_Q$ at In(2) with $M_{AF}^{max} = 8.7$ kOe and a linewidth broadening factor $\eta = 250$ kHz is shown by the solid line in Fig. 3a. The simulation for $1\nu_Q$ at In(1) with $M_{AF}^{max} = 2.7$ kOe and $\eta = 300$ kHz is also shown by the solid line in Fig. 3d. These simulations are in good agreement with their respective experimental results, indicating that M_{AF} is randomly distributed as illustrated in Fig. 3c.

Next, we discuss superconducting characteristics for CeIr(In_{0.925}Cd_{0.075})₅. The T dependences of $1/T_1$ normalized at T_c are shown for the pure and Cd-doped samples in Figs. 2(c) and 2(d), respectively. In general, the T dependence of $1/T_1$ below T_c allows us to estimate a superconducting gap ($2\Delta_0/k_B T_c$) and a residual density of states (RDOS) at the Fermi level due to some impurity effect by assuming a certain pairing symmetry. Here, we tentatively assume a $d_{x^2-y^2}$ -wave model which is indicated by the thermal-conductivity, magnetic-penetration-depth, and specific-heat measurements [20–22]. The solid lines in Figs. 2(c) are the calculated results for CeIrIn₅ with parameters of $(2\Delta_0/k_B T_c, \text{RDOS}) = (5.2, 0.44)$ at $P = 0$ and $(5.2, 0.66)$ at $P = 2.73$ GPa. Since RDOS in CeIrIn₅ are unexpectedly much larger than RDOS = 0.08 at $P = 0$ in CeCoIn₅ [6] and 0.14 at $P = 2.35$ GPa in CeRhIn₅ [23] in spite of its high purity, it is possible that a superconducting gap is not formed or is small enough to be easily broken even by weak impurity scattering in one or a few bands of the Fermi surface. Here, we highlight the fact that RDOS in CeIrIn₅ increases from 0.44 to 0.66 despite the enhancement of T_c from 0.4 to 0.9 K. Such a behavior contrasts with those in CeCoIn₅ and CeRhIn₅ in which RDOS remains almost unchanged and is reduced as P increases, respectively. The unconventional enhancement of RDOS by P cannot be understood in terms of a simple impurity effect. Analogous SC characteristics are also observed in the Cd-doped sample with the parameters of $(2\Delta_0/k_B T_c, \text{RDOS}) = (6.4, 0.64)$ and $(7.7, 0.73)$ at $P = 2.34$ and 2.75 GPa, respectively, indicating that it is intrinsic in the CeIr(In_{1-x}Cd_x)₅ system.

Since ν_Q depends directly on an electric field gradient at observed nuclei, probing a charge distribution emerging from surrounding ions and electrons, its P dependence is relevant with some changes in both the valence of Ce and a lattice volume. A structural phase transition is simply expected as one possible cause for an anomaly in the P dependence of ν_Q , but it is suggested from the x-ray diffraction measurements that no P -induced structural phase transition occurs up to 15 GPa in CeIrIn₅ [24]. We give an example of an anomaly in the P dependence of ν_Q in CeCu₂Si₂ relevant with the valence crossover. The NQR measurements under P in CeCu₂Si₂

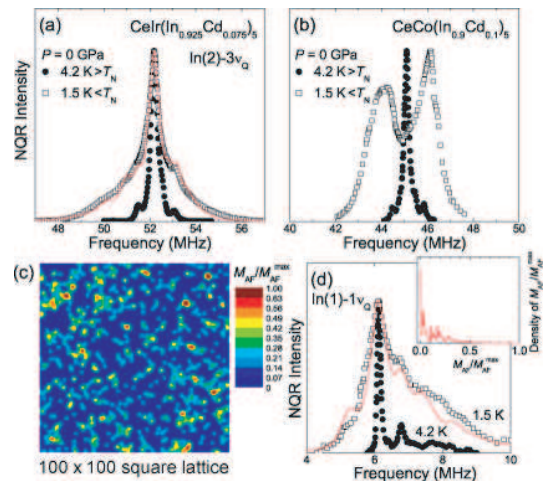


FIG. 3: (Color online) (a) The $3\nu_Q$ spectra at the In(2) site in CeIr(In_{0.925}Cd_{0.075})₅. The solid line is the calculated result (see text). (b) The $3\nu_Q$ spectra at the In(2) site in CeCo(In_{0.9}Cd_{0.1})₅. (c) Example of the M_{AF} distribution on a 100×100 square lattice calculated with randomly distributed 7.5% Cd dopants. (d) The $1\nu_Q$ spectrum at the In(1) site in CeIr(In_{0.925}Cd_{0.075})₅. The solid line is the calculated result (see text). The inset shows the density of M_{AF}/M_{AF}^{max} for a 500×500 square lattice.

reported that a change in the slope of the ν_Q versus P curve, $d\nu_Q/dP$ is observed around $P \sim 4.2$ GPa, just below where T_c reaches the maximum [12, 13]. It is suggested from the recent resistivity measurements that CeCu₂Si₂ lies in proximity to a valence transition: the critical end point between the first-order valence transition and valence crossover could be located at 4.5 ± 0.2 GPa and a slightly negative T [25]. Figure 4(b) indicates the P dependence of $2\nu_Q$ for the pure and Cd-doped samples. The P dependences of ν_Q closely resemble each other with a nearly 60 kHz gap between both samples. As shown in Fig. 4(b), ν_Q monotonously increases up to about 1 GPa, and $d\nu_Q/dP$ becomes steep above 1 GPa (see also Fig. 4(c)). It is noteworthy that T_N starts to decrease beyond 1 GPa, as confirmed in Fig. 4(a). This may be caused by the increase in the hybridization between Ce-4*f* and conduction electrons which triggers a change of the Ce valence above 1 GPa. As P increases further, $d\nu_Q/dP$ also increases around $P_v \sim 2.1$ GPa for both the samples, as shown in Fig. 4(b) and 4(c). Since SC2 suddenly emerges around P_v in the Cd-doped sample and the maximum of T_c is realized beyond P_v , it is likely that the anomaly of ν_Q at P_v is closely related with the Ce valence crossover inducing valence fluctuations as well as that for CeCu₂Si₂ under P [13]. It should be noted that the P variation of T_c around P_v in CeIrIn₅ is softer than that in CeCu₂Si₂, indicating that the valence crossover in CeIrIn₅ is not rapid, as compared to that in CeCu₂Si₂. Moreover, it is also expected that the unexpected enhancement of RDOS discussed before may arise from valence fluctuations. This is because the theory points out that valence fluctuations enhance impurity

scattering as observed in CeCu_2Si_2 [12]. In order to clarify the relation between the unexpected enhancement of RDOS and valence fluctuations, further theoretical work on the formation of a superconducting energy gap by valence fluctuations is clearly needed.

Next, we focus on an evolution of low-lying excitations which suddenly emerge above P_v in the Cd-doped sample. Fig. 2(b) indicates that the T dependences of $(T_1T)^{-1}$ below T_N are smoothly extrapolated from those well above T_N in $P = 0 - 1.90$ GPa below P_v , where SC is not induced. This result suggests that AFM moments around Cd dopants become static below T_N due to the formation of static IAF order because the enhancement in $(T_1T)^{-1}$ due to the AFM order appears only in the vicinity of T_N . However, once P exceeds P_v , the T dependences of $(T_1T)^{-1}$ below T_N are not extrapolated from those well above T_N , indicating that the low-lying excitations remaining even well below T_N may be responsible for the onset of SC2. A likely explanation for this unrecovered enhancement of $(T_1T)^{-1}$ is that magnetic moments are still fluctuating even below T_N through the development of valence fluctuations above P_v . Here, we emphasize that the stronger coupling effect in the Cd doped sample than in the pure one causes a comparable T_c with that in the pure one through the overcoming of a possible reduction of T_c due to the impurity effect and the induced IAF order. In this context, it is expected that the formation of strong coupling SC in the Cd doped sample is closely related to the low-lying excitations reinforced by valence fluctuations. Since the Cd-doping causes some change in the low-energy spin dynamics above P_v after all, further theoretical studies on a possible cooperative coupling between valence and spin fluctuations may be necessary to clarify the complicated mechanism of SC2 for the $\text{CeIr}(\text{In}_{1-x}\text{Cd}_x)_5$ system.

In conclusion, the present In-NQR measurements have revealed that SC2 in pure and Cd-doped CeIrIn_5 differs from SC1 that is closely related to the AFM correlation in many respects: the P dependence of ν_Q pointing to the valence change of Ce, the unexpected increase in RDOS by the application of P , and the unrecovered enhancement of $(T_1T)^{-1}$ even below T_N above P_v . These results lead us to consider that unconventional SC2 is likely mediated by valence fluctuations.

We thank S. Watanabe and K. Miyake for enlightening discussions and theoretical comments. This work was supported by Grants-in-Aid for Specially Promoted Research (No. 20001004), for Young Scientists (B) (No. 20740195), and for Scientific Research (C) (No. 24540372) from the Ministry of Education, Culture, Sports, Science and Technology (MEXT) of Japan. It was partially supported by the Global COE Program (No. G10) from MEXT.

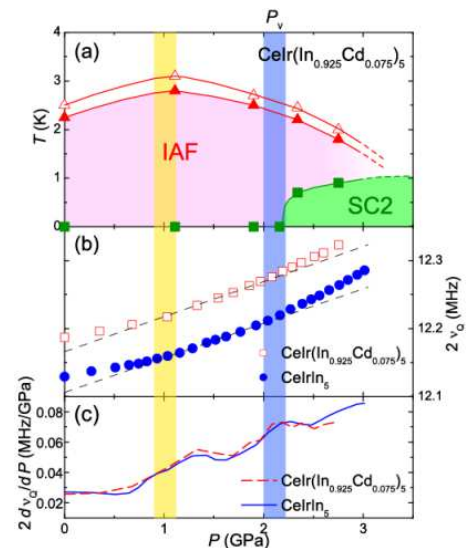


FIG. 4: (Color online) (a) The $P - T$ phase diagram for $\text{CeIr}(\text{In}_{0.925}\text{Cd}_{0.075})_5$. (b) The P dependences of $2\nu_Q$ for the In(1) site in CeIrIn_5 and $\text{CeIr}(\text{In}_{0.925}\text{Cd}_{0.075})_5$. The dashed lines are guides for the eyes. (c) The P dependences of $2d\nu_Q/dP$ obtained from Fig. 4(b). The values of $2d\nu_Q/dP$ are smoothed by a simple moving average with the nearest neighbors.

-
- [1] C. Petrovic, P. G. Pagliuso, M. F. Hundley, R. Movshovich, J. L. Sarrao, J. D. Thompson, Z. Fisk, and P. Monthoux, *J. Phys.: Cond. Mat.* **13**, L337 (2001).
 - [2] H. Hegger, C. Petrovic, E. G. Moshopoulou, M. F. Hundley, J. L. Sarrao, Z. Fisk, and J. D. Thompson, *Phys. Rev. Lett.* **84**, 4986 (2000).
 - [3] T. Muramatsu, N. Tateiwa, T. C. Kobayashi, K. Shimizu, K. Amaya, D. Aoki, H. Shishido, Y. Haga, and Y. Ōnuki, *J. Phys. Soc. Jpn.* **70**, 3362 (2001), and unpublished.
 - [4] C. Petrovic, R. Movshovich, M. Jaime, P. G. Pagliuso, M. F. Hundley, J. L. Sarrao, Z. Fisk, and J. D. Thompson, *Europhys. Lett.* **53**, 354 (2001).
 - [5] M. Nicklas, V. A. Sidorov, H. A. Borges, P. G. Pagliuso, J. L. Sarrao, and J. D. Thompson, *Phys. Rev. B* **70**, 020505(R) (2004).
 - [6] M. Yashima, S. Kawasaki, Y. Kawasaki, G.-q. Zheng, Y. Kitaoka, H. Shishido, R. Settai, Y. Haga and Y. Ōnuki, *J. Phys. Soc. Jpn.* **73**, 2073 (2004).
 - [7] M. Yashima, H. Mukuda, Y. Kitaoka, H. Shishido, R. Settai, and Y. Ōnuki, *Phys. Rev. B* **79**, 214528 (2009).
 - [8] S. Kawasaki, G.-q. Zheng, H. Kan, Y. Kitaoka, H. Shishido, and Y. Ōnuki, *Phys. Rev. Lett.* **94**, 037007 (2005).
 - [9] R. Borth, E. Lengyel, P. G. Pagliuso, J. L. Sarrao, G. Sparn, F. Steglich, and J. D. Thompson, *Physica B* **312-313**, 136 (2002).
 - [10] Y. Nakajima, H. Shishido, H. Nakai, T. Shibauchi, M. Hedo, Y. Uwatoko, T. Matsumoto, R. Settai, Y. Ōnuki, H. Kontani, and Y. Matsuda, *Phys. Rev. B* **77**, 214504 (2008).
 - [11] H. Q. Yuan, F. M. Grosche, M. Deppe, C. Geibel, G. Sparn, and F. Steglich, *Science* **302**, 2104 (2003).
 - [12] A. T. Holmes, D. Jaccard, and K. Miyake, *Phys. Rev. B*

- 69**, 024508 (2004).
- [13] K. Fujiwara, Y. Hata, K. Kobayashi, K. Miyoshi, J. Takeuchi, Y. Shimaoka, H. Kotegawa, T. C. Kobayashi, C. Geibel, and F. Steglich, *J. Phys. Soc. Jpn.* **77**, 123711 (2008).
- [14] Y. Onishi, and K. Miyake, *J. Phys. Soc. Jpn.* **69**, 3955 (2000).
- [15] S. Watanabe, M. Imada, and K. Miyake, *J. Phys. Soc. Jpn.* **75**, 043710 (2006).
- [16] K. Murata, K. Yokogawa, H. Yoshino, S. Klotz, P. Munsch, A. Irizawa, M. Nishiyama, K. Iizuka, T. Nanba, T. Okada, Y. Shiraga, and S. Aoyama, *Rev. Sci. Instrum.* **79**, 085101 (2008).
- [17] T. Moriya and K. Ueda, *Rep. Prog. Phys.* **66**, 1299 (2003).
- [18] L. D. Pham, T. Park, S. Maquilon, J. D. Thompson, and Z. Fisk, *Phys. Rev. Lett.* **97**, 056404 (2006).
- [19] R.R. Urbano, B.-L. Young, N. J. Curro, J. D. Thompson, L. D. Pham, and Z. Fisk, *Phys. Rev. Lett.* **99**, 146402 (2007).
- [20] Y. Kasahara, T. Iwasawa, Y. Shimizu, H. Shishido, T. Shibauchi, I. Vekhter, and Y. Matsuda, *Phys. Rev. Lett.* **100**, 207003 (2008).
- [21] D. Vandervelde, H. Q. Yuan, Y. Ōnuki, and M. B. Salamon, *Phys. Rev. B* **79**, 212505 (2009).
- [22] S. Kittaka, Y. Aoki, T. Sakakibara, A. Sakai, S. Nakatsuji, Y. Tsutsumi, M. Ichioka, and Kazushige Machida, *Phys. Rev. B* **85**, 060505(R) (2012).
- [23] M. Yashima, H. Mukuda, Y. Kitaoka, H. Shishido, R. Settai, and Y. Ōnuki, *Phys. Rev. B* **79**, 214528 (2009).
- [24] Ravhi S. Kumar, A. L. Cornelius, and J. L. Sarrao, *Phys. Rev. B* **70**, 214526 (2004).
- [25] G. Seyfarth, A.-S. Rüetschi, K. Sengupta, A. Georges, and D. Jaccard, *Europhys. Lett.* **98**, 17012 (2012).
- [26] G.-q. Zheng, N. Yamaguchi, H. Kan, Y. Kitaoka, J. L. Sarrao, P. G. Pagliuso, N. O. Moreno, and J. D. Thompson, *Phys. Rev. B* **70**, 014511 (2004).
- [27] S. Kawasaki, M. Yashima, Y. Mugino, H. Mukuda, Y. Kitaoka, H. Shishido, and Y. Ōnuki, *Phys. Rev. Lett.* **96**, 147001 (2006).